

Phase diagram of random lattice gases in the annealed limit

A. P. Vieira[†] and L. L. Gonçalves[‡]

Departamento de Física, Universidade Federal do Ceará

CP 6030, 60451-970 Fortaleza (CE) Brazil

[†] Present address: Instituto de Física, Universidade de São Paulo

CP 66318, 05315-970 São Paulo (SP) Brazil

[†] E-mail: apvieira@if.usp.br

[‡] E-mail: lindberg@fisica.ufc.br

January 7, 2018

Abstract

An analysis of the random lattice gas in the annealed limit is presented. The statistical mechanics of disordered lattice systems is briefly reviewed. For the case of the lattice gas with an arbitrary uniform interaction potential and random short-range interactions the annealed limit is discussed in detail. By identifying and extracting an entropy of mixing term, a correct physical expression for the pressure is explicitly given. The one-dimensional lattice gas with uniform long-range interactions and random short-range interactions satisfying a bimodal annealed probability distribution is discussed. The model is exactly solved and is shown to present interesting behavior in the presence of competition between interactions, such as the presence of three phase transitions with different critical temperatures and the occurrence of triple and quadruple points.

The lattice gas model [1] was introduced by Lee and Yang in 1952 as an application of their theory of condensation, due to its equivalence to the Ising model. Despite its somewhat artificial character, it has been extensively and successfully applied to the study of both solid-liquid and liquid-gas transitions [2]. It has also been applied to problems of adsorption of a gas on a crystal surface [3, 4, 5].

The mapping of the two-dimensional lattice gas with nearest-neighbor interaction into the Ising model in the square lattice allowed the exact calculation of the coexistence curve of a fluid transition exhibited by the lattice gas at sufficiently low temperatures. However, the corresponding equation of state could not be exactly determined, due to the absence of an exact solution for the Ising model in the presence of an external magnetic field. Such a solution exists for the one-dimensional analog of the model, although it undergoes no phase transition at finite temperature, having very little to contribute to even a qualitative analysis of the behavior of real substances.

Notwithstanding, in the presence of uniform infinite-range interactions phase transitions are induced even in one-dimensional systems [6]. Furthermore, as pointed out by Hemmer and Stell [7, 8], for lattice and continuous fluids in which the potential has both a long-range attraction and a short-range repulsion, plus a hard core, up to two phase transitions are expected. This is indeed verified for the $1d$ lattice gas with nearest-neighbor repulsion and long-range attraction [9, 10], described by the Hamiltonian

$$H = -4J \sum_{j=1}^N n_j n_{j+1} - \frac{4I}{N} \sum_{i,j=1}^N n_i n_j, \quad (1)$$

where $J < 0$, $I > 0$ and the occupation numbers $n_j \in \{0, 1\}$ represent the absence or presence of a particle in the j th site along the chain. Such model is mathematically equivalent to the Ising chain with short- and long-range interactions in an external field [11], which in turn is equivalent to a linear chain approximation for higher dimensional models. Depending on the ratio of the interaction parameters, the system can present one or two phase transitions, and in the latter case a triple point may be present [9, 10]. The three possible phases have zero-temperature densities given by $\rho = 0$ (gas phase), $\rho = \frac{1}{2}$ (liquid phase) and $\rho = 1$ (close-packed phase). However, the symmetry between unoccupied and occupied cells (hole-particle symmetry) [12] makes the critical temperatures for both transitions the same, differently from what happens in the analogous continuous model [9, 13].

On the other hand, for random versions of the model, by looking at ground state properties one can see that the presence of disorder in the nearest-neighbor interactions induces both the breaking of the hole-particle symmetry and the appearance of additional phase transitions at $T = 0$. Due to the presence of the long-range attraction those new transitions should persist at low but finite temperatures. It is then worthwhile examining disordered versions of the model and look for what new interesting properties may arise.

The main purpose of this paper is to study the phase diagram of the $1d$ lattice gas with random annealed nearest-neighbor interactions and uniform long-range interactions. This particular disordered version of the model 1 has the advantage of being exactly soluble. Although of difficult physical realization, it might be useful in studying adsorption problems, if one wishes to consider situations in which the presence of adsorbed particles induces diffusion of crystalline atoms in or near imperfect surfaces.

The outline of this paper is as follows. In order to clarify one subtle aspect of the mathematical treatment of annealed models, a preceding discussion is presented. Section 1 discusses some theoretical aspects of the statistical mechanics of disordered systems. The d -dimensional lattice gas with an arbitrary uniform interaction potential plus random short-range interactions is treated in Sec. 2, following the approach of Thorpe and Beeman for the Ising model [14]. The calculation of thermodynamic functions for this class of systems is presented, and a general method for calculating the equation of state is proposed. Then the one-dimensional lattice gas with random nearest-neighbor interactions and uniform long-range interactions is considered in Sec. 3. The main features of the behavior of the model are presented and discussed when the nearest-neighbor interactions are selected from a bimodal distribution. In the final section the conclusions and main results of the paper are summarized. The equivalence between the model and the random Ising model is presented in Appendix A, and in Appendix B the ground state properties of the model are discussed.

1 Disordered systems.

Disordered systems are characterized by two kinds of variables: dynamical variables, with mean relaxation time τ_h , and “structural” variables, related to the randomness of the system and with mean relaxation time τ_c . As introduced by Brout [15], there are two limits in which disorder problems can be formally treated, namely, the annealed and the quenched limits. The latter is appropriate to systems where disorder relaxes in a much longer time scale than dynamical variables ($\tau_c \gg \tau_h$), and so disorder variables can be considered as effectively frozen. The opposite situation, in which disorder and dynamical variables fluctuate in the same time scale ($\tau_c \approx \tau_h$), corresponds to the annealed limit. Since exact solutions can be found for some models, in these cases it is worthwhile using the annealed limit as an approximation to a quenched system, as it will be further discussed.

As shown by Mazo [16], the free energy of a random quenched system is given by

$$F_q = -k_B T \sum_{\{\kappa\}} p(\kappa) \ln Q(\kappa) + k_B T \sum_{\{\kappa\}} p(\kappa) \ln p(\kappa), \quad (2)$$

where k_B is Boltzmann's constant, T is the absolute temperature of the system, $p(\kappa)$ is the fixed probability of occurrence of the random configuration $\{\kappa\}$, $Q(\kappa)$ is the partition function of the system for that particular configuration, and the summations run over all possible configurations $\{\kappa\}$. The second summation in Eq.2 is interpreted as due to an entropy of mixing of the random variables. It is in general ignored, since the only way to measure an entropy is to change it, which is not possible in this case because the probabilities $p(\kappa)$ are rigid by assumption. Irrespective of that term, in general one finds that, for almost all thermodynamic functions obtained from the free energy by differentiation, the average value X_q of the function can also be calculated as an average of the corresponding values $X(\kappa)$ over all the disorder configurations,

$$X_q = \sum_{\{\kappa\}} p(\kappa) X(\kappa). \quad (3)$$

When lattice models are considered, disorder is usually represented by site or bond random variables. For example, in problems of adsorption of gas molecules on a crystal surface one may want to consider sites with random potentials or random interactions between particles in different adsorption sites. For simplicity, consider a lattice of N sites (or bonds). Suppose that some random variable κ_j can take one of M values $\{K_1, K_2, \dots, K_M\}$ at a given site (or bond) j with probability q_i , such that $\sum_{i=1}^M q_i = 1$. Since that probability is independent of the values of the other random variables in the system, the probability of a particular configuration $\{\kappa\} \equiv \{\kappa_1, \kappa_2, \dots, \kappa_N\}$ is given by

$$p(\kappa) = \prod_{i=1}^M q_i^{n_i}, \quad (4)$$

where n_i is the number of sites (or bonds) to which the value K_i of the random variable is associated in that given configuration $\{\kappa\}$. Obviously the n_i 's obey the constraint

$$\sum_{i=1}^M n_i = N. \quad (5)$$

It is possible to show that for this case the entropy of mixing in Eq.2 takes the form

$$-k_B \sum_{\{\kappa\}} p(\kappa) \ln p(\kappa) = -N k_B \sum_{i=1}^M q_i \ln q_i, \quad (6)$$

which is proportional to the volume of the system. So, if one keeps the entropy of mixing term and tries to calculate (in appropriate units) the pressure of a quenched lattice gas the result is

$$P_q = -\frac{\partial F_q}{\partial N} = k_B T \left[\sum_{\{\kappa\}} p(\kappa) P(\kappa) - \sum_{i=1}^M q_i \ln q_i \right], \quad (7)$$

where $P(\kappa)$ is the pressure calculated for a particular configuration $\{\kappa\}$. Clearly Eq.7 is a physically incorrect expression for the pressure, since in the zero density limit the first term vanishes, while the second term is positive. Furthermore, in the non-random limit ($K_i \equiv K$ for all i) all configurations are identical, but the entropy of mixing still contributes to the “pressure”. Finally the entropy of mixing diverges in the continuum limit ($M \rightarrow \infty, q_i \rightarrow 0$) [14]. Thus the correct expression for the pressure must lack the entropy of mixing, taking the form

$$P = k_B T \sum_{\{\kappa\}} p(\kappa) P(\kappa), \quad (8)$$

which is the expression used in previous studies of random lattice gases [17, 18]. The need to drop out the entropy of mixing in the calculation of the pressure of a quenched fluid was also pointed out by Singh and Kovac [19] on the basis of the interpretation of that term as an information entropy, introduced by Sobotta and Wagner [20].

For most systems the quenched limit is more realistic than the annealed limit, since in general $\tau_c \gg \tau_h$, as it happens in spin glasses, for instance. However, the exact mathematical treatment of the quenched limit is very difficult, due to the fact that the calculation of the free energy involves averaging logarithms of partition functions. On the other hand, the annealed free energy can be written in the form

$$F_a = -k_B T \ln Q_a \quad (9)$$

where Q_a denotes the average of the partition function over the disorder configurations. This is often calculated with the constraint that the thermal averages of the random variables obey some prescribed distribution, which is realized by the introduction of Lagrange multipliers playing the role of pseudo-chemical potentials. This implies that in the annealed limit the disorder variables are adjusted so as to minimize the free energy, a procedure which singles out a subset of the disorder configurations and introduces correlations between the disorder variables themselves. So, the annealed limit is in general not a good approximation to the quenched limit. Nevertheless, Morita [21] showed that a quenched system can be represented by a fictitious (annealed) equilibrium system subject to an additional potential, composed of an infinite series of Lagrange multipliers adjusted by the (quenched) n -“particle” correlation functions ($n = 1, 2, 3, \dots$) for the random variables. Indeed, for various Ising models it can be verified that by controlling correlations between pairs of random variables ($n = 2$) results for annealed systems approach those of the corresponding quenched systems [22, 23]. This treatment introduces mathematical difficulties which are of course increasingly greater, and so this work will analyze the usual case in which one tries to control only the concentration of the random variables ($n = 1$).

In the next section it will be shown that an entropy of mixing term can also be identified in a large class of annealed models, and must likewise be discarded in order to produce meaningful results.

2 Lattice gas with random short-range interactions: annealed limit.

Consider a N -site d -dimensional lattice gas model whose particles interact via an arbitrary uniform (non-random) potential plus short-range interactions satisfying the annealed probability distribution

$$\wp(\kappa_{ij}) = \sum_{k=1}^M q_k \delta(\kappa_{ij} - J_k), \quad (10)$$

for all pairs of nearest-neighbor sites i and j . The Hamiltonian of the model can be written as

$$H = H^{(U)} + \sum_{\langle i,j \rangle} H_{ij}, \quad (11)$$

where $H^{(U)}$ is the uniform term, the summation runs over all nearest-neighbor pairs of sites and

$$H_{ij} = - \sum_{k=1}^M \kappa_{ij} n_i n_j. \quad (12)$$

For any site i , variable $n_i = 0$ if the site is empty or $n_i = 1$ if the site is occupied by a particle.

Following the approach of Thorpe and Beeman for the Ising model [14], this situation can be formally treated by writing κ_{ij} in the form

$$\kappa_{ij} = \sum_{k=1}^M t_{ij,k} J_k, \quad (13)$$

and introducing M pseudo-chemical potentials ξ_k to control the averages of the random numbers $t_{ij,k}$, which for all (i, j) are subject to the constraints

$$t_{ij,k} \in \{0, 1\}, \quad \sum_{k=1}^M t_{ij,k} = 1, \quad \text{and} \quad \langle t_{ij,k} \rangle = q_k. \quad (14)$$

The annealed grand partition function of the system is given by

$$\mathcal{Z} = \sum'_{\{t\}} \exp \left[\beta \sum_{k=1}^M \xi_k \sum_{\langle i,j \rangle} t_{ij,k} \right] \sum_{\{n\}} \exp \left[\beta \mu \sum_{j=1}^N n_j - \beta H \right], \quad (15)$$

where the primed summation runs over those configurations satisfying the first two constraints in 14. After performing the partial trace over the random variables one obtains

$$\mathcal{Z} = \sum_{\{n\}} \exp \left[\beta \mu \sum_{j=1}^N n_j - \beta H^{(U)} \right] \prod_{\langle i,j \rangle} \left\{ \sum_{k=1}^M \exp [\beta (\xi_k + J_k n_i n_j)] \right\}. \quad (16)$$

Due to the fact that $n_i \in \{0, 1\}$ for all sites the term in braces in Eq.16 can be expressed as

$$\sum_{k=1}^M \exp [\beta (\xi_k + J_k n_i n_j)] \equiv A e^{K n_i n_j}, \quad (17)$$

if A and K are defined by the expressions

$$A = \sum_{k=1}^M w_k \quad \text{and} \quad e^K = \sum_{k=1}^M w_k e^{\beta J_k} / \sum_{k=1}^M w_k. \quad (18)$$

with $w_k \equiv \exp(\beta \xi_k)$. Equation 16 can now be written as

$$\mathcal{Z} = A^{Nq/2} \sum_{\{n\}} \exp \left[\beta \mu \sum_{j=1}^N n_j - \beta H^{(U)} + \sum_{\langle i,j \rangle} K n_i n_j \right] \equiv A^{Nq/2} \mathcal{Q}(K), \quad (19)$$

where q is the coordination number of the lattice and $\mathcal{Q}(K)$ is just the grand partition function of a regular lattice gas with short-range interaction energy K/β plus the uniform interaction potential.

The fugacities w_k are eliminated by imposing for all nearest-neighbor pairs (i, j) and all values of k the condition

$$\langle t_{ij,k} \rangle = q_k \Rightarrow \frac{w_k}{N} \frac{\partial \ln \mathcal{Z}}{\partial w_k} = q_k, \quad (20)$$

which can be rewritten as

$$w_k \frac{\partial \ln A}{\partial w_k} + \epsilon(K) w_k \frac{\partial K}{\partial w_k} = q_k, \quad (21)$$

where

$$\epsilon(K) \equiv \langle n_i n_j \rangle_K = \frac{2}{Nq} \frac{\partial \ln \mathcal{Q}(K)}{\partial K} \quad (22)$$

is the nearest neighbor pair correlation function for the regular lattice gas with interaction K/β . By rearranging terms in Eq.21 and imposing the condition $\sum_{k=1}^M q_k = 1$ one obtains

$$\sum_{k=1}^M \frac{q_k}{\coth \left[\frac{1}{2}(K - \beta J_k) \right] + 1 - 2\epsilon(K)} = 0, \quad (23)$$

which determines K if one is able to calculate $\epsilon(K)$. Notice that in general the effective interaction K/β depends on the temperature.

The density of the gas is set by the condition

$$\rho = \frac{z}{N} \frac{\partial \ln \mathcal{Z}}{\partial z} = \frac{z}{N} \frac{\partial \ln \mathcal{Q}(K)}{\partial z}, \quad (24)$$

and from this equation it is possible to eliminate the fugacity z .

The annealed free energy is given by [24]

$$f_a = -k_B T \left[\frac{1}{N} \ln \mathcal{Z} - \sum_{k=1}^M q_k \ln w_k - \rho \ln z \right], \quad (25)$$

which after straightforward calculations can be written in the form

$$f_a = f_K - k_B T \left\{ \sum_{k=1}^M q_k \ln [1 - \epsilon(K) (1 - e^{\beta J_k - K})] - \sum_{k=1}^M q_k \ln q_k \right\}, \quad (26)$$

where

$$f_K = -k_B T \left[\frac{1}{N} \ln \mathcal{Q}(K) - \rho \ln z \right] \quad (27)$$

is the free energy of the regular system. The last summation on the right hand side of Eq.26 is an entropy of mixing term, identical to that in Eq.7, and must be dropped as discussed in Sec.1. With that correction, the free energy per lattice site takes the form

$$f = f_K - k_B T \sum_{k=1}^M q_k \ln [1 - \epsilon(K) (1 - e^{\beta J_k - K})], \quad (28)$$

and the pressure of the system can then be calculated from the thermodynamic relation

$$P = \rho\mu - f = k_B T \rho \ln z - f \Rightarrow \quad (29)$$

$$\Rightarrow P = k_B T \left\{ \frac{1}{N} \ln \mathcal{Q}(K) + \sum_{k=1}^M q_k \ln [1 - \epsilon(K) (1 - e^{\beta J_k - K})] \right\}, \quad (30)$$

the first term being just the pressure of the regular lattice gas with effective interaction K/β . In the non-random limit ($J_k \equiv J$ for all k) Eq.23 gives $K = \beta J$ and according to Eq.30 the pressure is given by

$$P \equiv P_K = \frac{k_B T}{N} \ln \mathcal{Q}(K), \quad (31)$$

which is obviously the correct expression.

From the results of this section it is then clear that, as in the quenched limit, the entropy of mixing term can be made explicit in the free energy of any lattice gas with annealed short-range interactions, and that the correct equation of state can be obtained by discarding that term. This is a fairly general result and will be applied in the next section to the $1d$ lattice gas with random nearest-neighbor and uniform long-range interactions.

3 One-dimensional lattice gas with random short-range interactions and uniform long-range interactions: annealed limit.

The existence of exact solutions [9, 10] for the uniform model 1 allows one to exactly solve the model in the presence of random annealed nearest-neighbor interactions, as shown in the previous section.

The Hamiltonian of a $1d$ lattice gas with uniform long-range interactions and random nearest-neighbor interactions is given by

$$H = -4 \sum_{j=1}^N \kappa_j n_j n_{j+1} - \frac{4I}{N} \sum_{i,j} n_i n_j, \quad (32)$$

where the nearest-neighbor interactions κ_j satisfy the annealed distribution

$$\wp(\kappa_j) = \sum_{k=1}^M q_k \delta(\kappa_j - J_k). \quad (33)$$

The thermodynamic properties of this random model can be obtained from those of a reference system without the long-range interactions. In particular the Helmholtz free energy is given by [6]

$$f(\rho, T) = \text{CE} \left[\tilde{f}(\rho, T) - 4I\rho^2 \right], \quad (34)$$

where $\tilde{f}(\rho, T)$ is the free energy of the reference system as a function of the density ρ and temperature T , while ‘‘CE’’ denotes the convex envelope of the function in square brackets. Correspondingly, the pressure P and chemical potential μ are given by [6]

$$P = \text{MC} \left[\tilde{P} - 4I\rho^2 \right], \quad \mu = \tilde{\mu} - 8I\rho, \quad (35)$$

where ‘‘MC’’ denotes the Maxwell construct of the function in square brackets and

$$\tilde{P} = \rho\tilde{\mu} - \tilde{f}(\rho, T) \quad \text{and} \quad \tilde{\mu} = \frac{\partial \tilde{f}}{\partial \rho} \quad (36)$$

are the corresponding functions for the reference system.

From the results of the previous section, Eqs.28 and 30, the free energy \tilde{f} and pressure \tilde{P} of the reference system without long-range interaction are given in terms of the corresponding functions \tilde{f}_K and \tilde{P}_K for a regular model with effective nearest-neighbor interaction K/β . The grand-partition function of this regular model is given by

$$\tilde{Q}(K) = \sum_{\{n\}} \exp \left[\beta\tilde{\mu} \sum_{j=1}^N n_j + K \sum_{j=1}^N n_j n_{j+1} \right], \quad (37)$$

and by using the transfer matrix method with cyclic boundary conditions one easily finds

$$\beta\tilde{P}_K = \frac{1}{N} \ln \tilde{Q}(K) = \ln \frac{1}{2} \left\{ 1 + \tilde{z}e^{4K} + \left[(1 - \tilde{z}e^{4K})^2 + 4\tilde{z} \right]^{1/2} \right\}, \quad (38)$$

where $\tilde{z} \equiv \exp(\beta\tilde{\mu})$. The density of the system is then given by the relation

$$\rho = \frac{\partial \tilde{P}_K}{\partial \tilde{\mu}} = \tilde{z} \left\{ \frac{e^{4K} - [(1 - \tilde{z}e^{4K})e^{4K} - 2] \left[(1 - \tilde{z}e^{4K})^2 + 4\tilde{z} \right]^{-1/2}}{1 + \tilde{z}e^{4K} + \left[(1 - \tilde{z}e^{4K})^2 + 4\tilde{z} \right]^{1/2}} \right\}, \quad (39)$$

from where the fugacity \tilde{z} of the reference system can be determined, and the nearest-neighbor pair correlation function of the regular system is given by

$$\epsilon(K) = \frac{\partial (\beta\tilde{P}_K)}{\partial K} = \tilde{z}e^{4K} \left\{ \frac{1 - (1 - \tilde{z}e^{4K}) \left[(1 - \tilde{z}e^{4K})^2 + 4\tilde{z} \right]^{-1/2}}{1 + \tilde{z}e^{4K} + \left[(1 - \tilde{z}e^{4K})^2 + 4\tilde{z} \right]^{1/2}} \right\}. \quad (40)$$

Finally, the pressure of the random system with long-range interactions described by the Hamiltonian in Eq.32 is

$$P = \text{MC} \left\{ \tilde{P}_K + k_B T \sum_{k=1}^M q_k \ln [1 - \epsilon(K) (1 - e^{4\beta J_k - 4K})] - 4I\rho^2 \right\}, \quad (41)$$

with K determined from the solution of Eq.23. So, the complete equation of state can be obtained from Eqs.38-41.

An alternative approach can be used to solve this problem, namely, the mapping onto the random Ising model. This is discussed in Appendix 4 and has the advantage of making evident the breaking of hole-particle symmetry. Furthermore, it provides a way of avoiding the use of the Maxwell construct by previously locating free energy minima, which directly indicate phase transitions.

The results above are applied to the case in which the nearest-neighbor interactions are selected from the bimodal distribution

$$\wp(\kappa_j) = p\delta(\kappa_j - J_A) + (1 - p)\delta(\kappa_j - J_B), \quad (42)$$

where the interactions J_B are assumed repulsive ($J_B < 0$). This is done in order to introduce competition effects, which, as in the pure model, are responsible for complex behavior. In the absence of competition between short- and long-range interactions the system presents at most one phase transition. The ground state properties of the model, discussed in detail in Appendix 4, indicate that at $T = 0$ and for $J_A \neq 0$ the system undergoes at most three phase transitions. For $J_A > 0$, when there is competition between the nearest-neighbor interactions, at fixed pressure the system can present itself in structures characterized by $\rho = 0$ (gas phase), $\rho = p$, $\rho = \frac{1}{2}(1+p)$ (liquid phases), and $\rho = 1$ (close-packed phase). For $J_A < 0$ all nearest-neighbor interactions are repulsive, and the stable phases are those for which $\rho = 0$ (gas), $\rho = \frac{1}{2}$, $\rho = \frac{1}{2}(1+p)$ (liquid phases) and $\rho = 1$ (close-packed). For $J_A = 0$ the system undergoes at most two transitions, associated with those of the pure model [9, 10], the liquid-phase density being shifted to $\rho = \frac{1}{2}(1+p)$.

The characterization of the phases $\rho = \frac{1}{2}$, $\rho = p$ and $\rho = \frac{1}{2}(1+p)$ as liquid phases is based on the instability of the corresponding structures. As in the uniform case, the $\rho = \frac{1}{2}$ phase at $T = 0$ is stable at certain pressures because particles are forced by nearest-neighbor repulsion to occupy every other site of the lattice. At any finite temperature, thermal fluctuations overcome the effect of the repulsion, inducing local fluctuations of the density and destroying the structure. The stability of the $\rho = p$ and $\rho = \frac{1}{2}(1+p)$ phases at $T = 0$, on the other hand, is related to the existence of interaction domains (Appendix 4). These are a consequence of the interactions mobility in the annealed limit and are formed as particles are added to the system at fixed volume in order to minimize the free energy. In the $\rho = p$ phase all sites in the J_A domains are occupied, while all those in J_B domains are empty. For $\rho = \frac{1}{2}(1+p)$ all sites in J_A domains and every other site in J_B domains are occupied. However, interaction domains are also destroyed by thermal fluctuations at any finite temperature, making the corresponding structures unstable.

In the following subsections the properties of the model at all temperatures are discussed for the various possible cases. The relevant parameters are renormalized by $|J_B|$,

$$\delta \equiv \frac{J_A}{|J_B|}, \quad \alpha \equiv \frac{I}{|J_B|}, \quad \theta \equiv \frac{k_B T}{|J_B|}, \quad P^* = \frac{P}{|J_B|}. \quad (43)$$

In passing it should be mentioned that, for repulsive long-range interaction ($I < 0$), the system does not undergo a phase transition irrespective of the sign of the short-range interaction.

3.1 Case $J_A = 0$.

For dilute short-range interactions there are at most two phase transitions, whose critical temperatures are different for $p \in (0, 1)$ because of the breakdown of hole-particle symmetry, as already stated. The critical temperature T_c of the gas-liquid (G-L) transition is always higher than T'_c , the critical temperature of the liquid-close-packed (L-CP) transition. This is in agreement to what is verified for the corresponding non-random continuum model [9, 13], in which there is no hole-particle symmetry.

For $p \neq 1$ there is always a range of values of α in which one or two triple points exist, as can be seen from the reentrant behavior of the triple point temperature (T_t) curves in the $T \times \alpha$ diagrams of Figs. 1(a)-(c), for $p = 0.1$, $p = 0.25$ and $p = 0.5$, respectively. The critical temperature of the G-L transition coincides with the triple point temperature for $\alpha = \alpha_{ct}$, whose dependence on p is shown in Fig. 1(d). It can be seen that α_{ct} approaches $\alpha_{tr} \simeq 3.1532$ as $p \rightarrow 0$, while for $p \rightarrow 1$, where there is no short-range repulsion, α_{ct} approaches $\alpha_0 = 2$. This is the value of α for which T_t vanishes for all p when $J_A = 0$.

Examples of the behavior of the isotherms and phase diagrams for $p = 0.1$ are shown in Figs. 2-4. In Fig. 2, for $\alpha = 1.5$, there are two-phase transitions even at $T = 0$ and there is no triple point. For low

temperatures the derivative of the L-CP transition pressure with respect to T is negative. This is related to the destruction by thermal fluctuations of the interaction domains built at $T = 0$, which makes the effective short-range repulsion weaker, lowering the pressure needed to pack the particles. In Fig. 3, for $\alpha = 2.2$, there is only one phase transition (G-CP) at $T = 0$, although two transitions occur for a range of temperatures above the triple point. In Fig. 4, for $\alpha = \alpha_{ct} \simeq 2.4297$, the critical temperature of the L-CP transition coincides with the triple point temperature, and for $\alpha > \alpha_{ct}$ there is only one phase transition. The behavior of the system when there are two triple points will be exemplified in the next subsection.

3.2 Case $J_A > 0$.

When there is competition between short-range interactions even a small amount of randomness is responsible for interesting behavior, as can be seen in the $\rho \times T$ projection of the coexistence surfaces shown in Figs. 5(a) and (b) for $J_A = -J_B$ ($\delta = 1$), $p = 0.07$ and two slightly different values of α . In both cases there are three phase transitions at $T = 0$, defining in decreasing density the close-packed, the two liquid (L_1 and L_2) and the gas phases. The lowest critical temperature corresponds to a L_2 -G transition. Above that there is an intermediate range of temperatures in which the system presents only two transitions. For $\alpha = 1.13$ that range is limited by a triple point, immediately above whose temperature there is again three phase transitions, as shown in Fig. 5(a). But for $\alpha = 1.129$ that triple point is replaced by another critical point, giving rise to a coexistence “bubble”, as can be seen in Figs. 5(b). The $T \times \alpha$ diagram for $\delta = 1$ and $p = 0.07$ is shown in Fig. 6. When the long-range attraction is sufficiently weak the system can present three phase transitions, whose critical temperatures are shown as solid lines in the figure. Triple points (broken lines) are present for intermediate values of α . The breaking and the reentrant behavior of the T_c curve, evident in the inset of Fig. 6, is related to the appearance of coexistence “bubbles”. That unusual behavior is observed only for values of p between $p \simeq 0.06$ and $p \simeq 0.08$.

The system may also present a quadruple point, i.e. coexistence of four phases, if $J_A > -J_B$ ($\delta > 1$). This is exemplified for $\delta = 2$ and $p = 0.1$ in the $T \times \alpha$ diagram in Fig. 7, where four triple point curves (dotted lines) intersect at the quadruple point P_q . Figures 8 and 9 show $P \times T$ and $\rho \times T$ diagrams for $\delta = 2$, $p = 0.08$ and values of α around α_q , illustrating the possible existence of two triple points or a quadruple point.

3.3 Case $J_B < J_A < 0$.

As detailed in Appendix B, when all short-range interactions are repulsive the possible structures at $T = 0$ correspond to $\rho = 1$ (close-packed phase), $\rho = \frac{1}{2}(1 + p)$ (liquid-1 phase), $\rho = \frac{1}{2}$ (liquid-2 phase) and $\rho = 0$ (gas phase).

When $|J_B|$ is much larger than $|J_A|$ the behavior of the system is expected to be similar to the dilute case ($J_A = 0$). This is confirmed for the case $J_A = \frac{3}{10}J_B$ ($\delta = -\frac{3}{10}$), as shown in the $\theta \times \alpha$ diagrams in Figs. 10(a)-(c) and the $\alpha \times p$ diagram in Fig. 10(d). Except for the presence of three phase transitions for small values of α , the behavior is similar to that observed in Fig. 1. Isotherms and phase diagrams are shown in Figs. 11 and 12 for $p = 0.5$, $\alpha = 0.8$ and $p = 0.75$, $\alpha = 0.8$, respectively. As expected for $\delta > -\frac{1}{2}$ (see Appendix B) the two-transition regime at $T = 0$ consist of the $\rho = 0$, $\rho = \frac{1}{2}(1 + p)$ and $\rho = 1$ phases, as in the dilute case. For small values of the long-range interactions, the great energy difference between short-range interactions leads to the high pressure needed to close-pack the system, when it is necessary to occupy nearest neighbor sites with J_B bonds. At low pressure the occupation of those sites is virtually forbidden, giving rise to the behavior shown in Figs. 11 and 12. As the value of α is increased, the system becomes more similar to the dilute case, as can be seen in Figs. 10(a)-(c).

When $\frac{1}{2}|J_B| < |J_A| < \frac{2}{3}|J_B|$ ($-\frac{2}{3} < \delta < -\frac{1}{2}$) both two-transition regimes at $T = 0$, described in Appendix B are possible, with the liquid-phase corresponding to $\rho = \frac{1}{2}$ or $\rho = \frac{1}{2}(1+p)$ if p is less or greater than $p' \equiv (1+2\delta)/(1+\delta)$, respectively. At finite temperatures the case $p = p'$ contains ingredients of both regimes. The $\theta \times \alpha$ diagram for the case $J_A = \frac{3}{5}J_B$ ($\delta = -\frac{3}{5}$) and $p = p' = \frac{1}{2}$ is shown in Fig. 13. Notice that both triple point lines touch the α axis at the same point, indicating the absence of a two-transition regime at $T = 0$. Figure 14 shows isotherms and phase diagrams for the same case and $\alpha = 1.45$, where a triple point is observed, corresponding to the coexistence of the close-packed and the two liquid phases. The L_1 - L_2 transition line has a positive temperature derivative, as shown in Fig. 14(b), differently from what is observed for $\delta > 0$, as shown in Fig. 8(a).

For $p < p'$ and in the two-transition regime, the $T = 0$ liquid-close-packed transition pressure is given by $P = -4[pJ_A + (1-p)J_B + I]$, the arithmetic mean of the corresponding results for the pure cases $p = 0$ and $p = 1$. For $p > p'$ the system can present a quadruple point, as observed for the $\delta > 1$ case.

4 Conclusions.

The Helmholtz free energy of any lattice gas model with random short-range interactions in the annealed limit was shown to present an entropy of mixing term. As shown for the quenched limit, that term has to be dropped from the free energy in order to give correct physical expressions for the pressure.

As an application, the one-dimensional lattice gas with uniform infinite range interactions and random short-range interactions satisfying bimodal distributions was exactly solved. Explicit results were presented for the cases $J_A = 0$, $J_A = -J_B > 0$, $J_A = -2J_B > 0$, $J_A = \frac{3}{10}J_B < 0$ and $J_A = \frac{3}{5}J_B < 0$, where there is competition between short- and long-range interactions. In general, the system can present at most three phase transitions at a fixed temperature. The phases were identified as close-packed, gas and two liquid phases, the latter being characterized at low temperatures by the existence of interaction domains. A very important effect of disorder was the breaking of the hole-particle symmetry of the pure model, which induces different critical temperatures for the transitions. Under certain conditions phase diagrams present negative thermal derivatives of some transition pressures, a phenomenon observed in nature in water, for instance. The existence of triple and quadruple points was demonstrated, and for $J_A > 0$ and small values of p the existence of coexistence “bubbles” was observed.

Appendix A. Equivalence between the random lattice gas and the random Ising model.

Here an alternative treatment for the problem of the random lattice gas discussed in Sec. 3 is presented.

By using the transformation [1]

$$n_j = (1 - \sigma_j)/2, \quad \sigma_j = \pm 1, \quad (44)$$

it can be shown that the annealed grand partition function of the random lattice gas,

$$\mathcal{Z} = \sum'_{\{t\}} \exp \left[\beta \sum_{k=1}^M \xi_k \sum_{j=1}^N t_{j,k} \right] \sum_{\{n\}} \exp \left[\beta \mu \sum_{j=1}^N n_j - \beta H \right], \quad (45)$$

can be written as

$$\mathcal{Z} = \exp \left[-N \left(\bar{h} + 2 \sum_{k=1}^M q_k J_k + \bar{I} \right) \right] Z_\sigma, \quad (46)$$

where $\bar{I} \equiv \beta I$, $\bar{h} \equiv \beta h = -2\bar{I} - \frac{1}{2}\beta\mu$ and

$$Z_\sigma = \sum_{\{t,\sigma\}} \exp \left[\beta \sum_{j=1}^N \sum_{k=1}^M t_{j,k} \left(\tilde{\xi}_k + J_k \sigma_j \sigma_{j+1} \right) + \frac{\bar{I}}{N} \sum_{i,j=1}^N \sigma_i \sigma_j + \sum_{j=1}^N \tilde{h}_j \sigma_j \right] \quad (47)$$

is the annealed grand partition function of a random Ising model with

$$\tilde{\xi}_k = \xi_k + J_k \quad (48)$$

and

$$\tilde{h}_j \equiv \bar{h} + 2\beta \sum_{k=1}^M [q_k - t_{j,k}] J_k. \quad (49)$$

Notice that the distributions of the random fields \tilde{h}_j and the short-interactions κ_j are correlated. The presence of the random terms in the effective field \tilde{h}_j acting on the spin in the j th site breaks the $h \rightarrow -h$, $\{\sigma\} \rightarrow \{-\sigma\}$ symmetry present in the uniform Ising model (for which $J_k \equiv J$ for all k). The effect of this on the behavior of the gas is that, unlike the pure model, the hole-particle symmetry is also broken in the presence of any randomness, and so all transitions have different critical temperatures. This is in contrast to the lattice gas with particles interacting via softened core uniform potentials [7, 8], where multiple phase transitions are also present, but whose critical temperatures are not all different because the symmetry is still present.

The correlation between the random fields and random interactions allows one to perform the partial trace over the disorder variables, mapping the system onto a regular Ising model with an effective interaction K/β and a interaction dependent effective field. Rewriting Eq.47 as

$$Z_\sigma = \sum_{\{\sigma\}} \hat{Z}(\sigma) \prod_{j=1}^N \left\{ \sum_{k=1}^M \exp \left[\beta J_k (\sigma_j \sigma_{j+1} - \sigma_j - \sigma_{j+1}) + \beta \tilde{\xi}_k \right] \right\}, \quad (50)$$

where

$$\hat{Z}(\sigma) \equiv \exp \left[\frac{\bar{I}}{N} \sum_{i,j=1}^N \sigma_i \sigma_j + \left(\bar{h} + 2\beta \sum_{k=1}^M q_k J_k \right) \sum_{j=1}^N \sigma_j \right], \quad (51)$$

and performing a decimation

$$\prod_{j=1}^N \left\{ \sum_{k=1}^M \exp \left[\beta J_k (\sigma_j \sigma_{j+1} - \sigma_j - \sigma_{j+1}) + \beta \tilde{\xi}_k \right] \right\} \equiv A e^{K(\sigma_j \sigma_{j+1} - \sigma_j - \sigma_{j+1})}, \quad (52)$$

with

$$A^4 = \left(\sum_{k=1}^M \tilde{w}_k e^{3\beta J_k} \right) \left(\sum_{k=1}^M \tilde{w}_k e^{-\beta J_k} \right)^3, \quad (53)$$

$$e^{4K} = \left(\sum_{k=1}^M \tilde{w}_k e^{3\beta J_k} \right) / \left(\sum_{k=1}^M \tilde{w}_k e^{-\beta J_k} \right) \quad (54)$$

and

$$\tilde{w}_k \equiv \exp\left(\beta\tilde{\xi}_k\right),$$

one can express the annealed grand-partition function Z_σ as

$$Z_\sigma = A^N \sum_{\{\sigma\}} \exp\left[K \sum_{j=1}^N \sigma_j \sigma_{j+1} + \frac{\bar{I}}{N} \sum_{i,j=1}^N \sigma_i \sigma_j + \tilde{h} \sum_{j=1}^N \sigma_j\right], \quad (55)$$

where

$$\tilde{h} \equiv \bar{h} + 2 \left(\bar{I}\sigma + \beta \sum_{k=1}^M q_k J_k - K \right). \quad (56)$$

By eliminating A and the fugacities \tilde{w}_k the annealed free energy of the random Ising model (as a function of the magnetization) can be written as

$$\begin{aligned} f_\sigma &= f(K, \sigma) + k_B T \sum_{k=1}^M q_k \ln q_k + \\ &+ k_B T \sum_{k=1}^M q_k \ln \frac{4e^{K-\beta J_k}}{[3 - \epsilon(K)]e^{2(K-\beta J_k)} + [1 + \epsilon(K)]e^{-2(K-\beta J_k)}}, \end{aligned} \quad (57)$$

in which once more there is an entropy of mixing term and

$$f(K, \sigma) \equiv -k_B T \ln \left\{ e^K \left[\cosh \tilde{h} + \left(\sinh^2 \tilde{h} + e^{-4K} \right)^{1/2} \right] \right\} + I\sigma^2 \quad (58)$$

is the free energy of an Ising model with average magnetization σ in a uniform field and uniform short- (K/β) and long-range (I) interactions [10], K being determined from the solution of the equation

$$\sum_{k=1}^M \frac{q_k}{2 \coth[2(K - \beta J_k)] + [1 - \epsilon_\sigma(K)]} = 0. \quad (59)$$

The nearest-neighbor spin-spin correlation function is explicitly given by

$$\epsilon_\sigma(K) \equiv \langle \sigma_j \sigma_{j+1} \rangle_K = 1 - \frac{2e^{-4K} \left(\sinh^2 \tilde{h} + e^{-4K} \right)^{-1/2}}{\cosh \tilde{h} + \left(\sinh^2 \tilde{h} + e^{-4K} \right)^{1/2}}. \quad (60)$$

By inverting the transformation 44 the annealed free energy of the lattice gas can be written as

$$f_g = -\frac{k_B T}{N} \ln \mathcal{Z} + \sum_{k=1}^M q_k \xi_k + \rho\mu = \left(h + \sum_{k=1}^M q_k J_k + I \right) + f_a + \rho\mu, \quad (61)$$

from where the pressure is calculated by explicitly excluding the entropy of mixing term present in f_a ,

$$P = \rho\mu - f_g + k_B T \sum_{k=1}^M q_k \ln q_k \Rightarrow$$

$$\Rightarrow P = - \left(h + \sum_{k=1}^M q_k J_k + I \right) - f_\sigma + k_B T \sum_{k=1}^M q_k \ln q_k, \quad (62)$$

while the density is given by

$$\rho = \frac{1 - \sigma}{2}. \quad (63)$$

By studying the properties of the Ising model described by the free energy f_σ in Eq.57 the behavior of the lattice gas can be determined. The equilibrium state of the magnetic system at fixed temperature and external field h is that which minimizes f_σ . By locating those minima and using Eqs.62 and 63 the equation of state of the gas is exactly determined. This procedure automatically removes the unstable portions of the isotherms and is equivalent to the Maxwell construct.

Appendix B. Ground state properties.

At zero temperature the Helmholtz free energy F of a system is identical to its internal energy, as it is evident from the thermodynamic relation

$$F = E - TS, \quad (64)$$

where T is the temperature and S is the entropy.

The ground state behavior of the system can thus be determined by writing the internal energy E for the various ranges of the density ρ and calculating the pressure using the expression

$$P|_{T=0} = \text{MC} \left[\rho \frac{\partial E}{\partial \rho} - E \right], \quad (65)$$

where ‘‘MC’’ denotes the Maxwell construct [6] of the function in square brackets, which substitutes horizontal parts (corresponding to phase transitions) for the unstable portions of the isotherms.

A fundamental feature of annealed models is that impurities are free to rearrange themselves so as to minimize the free energy. For a lattice gas with random interactions this means that, as particles are added to the system, interactions of the same kind have a tendency to aggregate, forming domains. From this analysis it is possible to find those structures which minimize the internal energy and determine the ground state behavior of the model discussed in Sec. 3, which is summarized below. In the following discussion the volume of the system is regarded as fixed.

Case $J_B < 0 \leq J_A$. In this situation, because of the presence of the attractive interactions J_A , interaction domains are formed even at infinitesimal densities. For sufficiently weak long-range attraction energy I , the density can be increased from $\rho = 0$ to $\rho = p$ at zero pressure by adding particles to the J_A domains. At densities between $\rho = p$ and $\rho = \frac{1}{2}(1 + p)$ new particles can be allocated with minimum energy cost at every other site of the J_B domains. The pressure is nevertheless raised, because of the smaller volume available. Finally, for $\rho > \frac{1}{2}(1 + p)$ particles can be added only by allocating them in empty sites between two other particles in the J_B domain, raising both internal energy and pressure. For strong long-range attraction some

of the transitions are suppressed, the various possibilities for the $T = 0$ isotherms being as follows.

$$\left\{ \begin{array}{l} \mathbf{3 \text{ transitions:}} \\ \left\{ \begin{array}{l} 0 < \rho < p, \quad P = 0 \equiv P_1 \\ p < \rho < \frac{1}{2}(1+p), \quad P = 4pJ_A - 2p(1+p)I \equiv P_2 \\ \frac{1}{2}(1+p) < \rho < 1, \quad P = 4[pJ_A - (1-p)J_B] - 2(1+p)I \equiv P_3 \end{array} \right. \\ \text{condition: } I < \min \left\{ -\frac{2}{1+p}J_B, \frac{2}{1+p}J_A \right\} \end{array} \right.$$

$$\left\{ \begin{array}{l} \mathbf{2 \text{ transitions:}} \\ \left\{ \begin{array}{l} 0 < \rho < \frac{1}{2}(1+p), \quad P = P_1 \\ \frac{1}{2}(1+p) < \rho < 1, \quad P = P_3 \end{array} \right. \\ \text{conditions: } \left\{ \begin{array}{l} p > \frac{J_A+J_B}{J_A-J_B} \equiv p_d \quad \text{and} \\ \frac{2}{1+p}J_A < I < 2 \left[\frac{p}{1+p}J_A - J_B \right] \end{array} \right. \end{array} \right.$$

$$\left\{ \begin{array}{l} \mathbf{2 \text{ transitions:}} \\ \left\{ \begin{array}{l} 0 < \rho < p, \quad P = P_1 \\ p < \rho < 1, \quad P = 4p(J_A - J_B - I) = P'_2 \end{array} \right. \\ \text{conditions: } \left\{ \begin{array}{l} J_A > -J_B \quad \text{and} \\ p < p_d \quad \text{and} \\ -\frac{2}{1-p}J_B < I < J_A - J_B \end{array} \right. \end{array} \right.$$

$$\left\{ \begin{array}{l} \mathbf{1 \text{ transition:}} \\ \{0 < \rho < 1, \quad P = P_1 \\ \text{conditions: } \left\{ \begin{array}{l} p < p_d \quad \text{and} \quad I > J_A - J_B \\ \text{or} \\ p > p_d \quad \text{and} \quad I > 2 \left[\frac{p}{1+p}J_A - J_B \right] \end{array} \right. \end{array} \right.$$

Case $J_B < J_A < 0$. This is the case where all nearest-neighbor interactions are repulsive. For sufficiently weak long-range interactions I there is no aggregation of particles at low densities. On the contrary, particles can be added to the system at minimum cost by allocating them such that they have no nearest neighbors. In general this can be done at zero pressure only if $\rho < \frac{1}{2}$. For greater densities interaction domains are formed, and new particles are allocated, by raising the pressure, between occupied sites in the J_A domains, which are filled up for $\rho = p + \frac{1}{2}(1-p) = \frac{1}{2}(1+p)$. Adding further particles requires even higher pressures, since they must occupy available sites in the J_B domains. Again the existence of the various possible transitions

depends on the strength of the long-range interactions. Zero temperature isotherms are described below.

$$\left\{ \begin{array}{l} \mathbf{3 \text{ transitions:}} \\ \left\{ \begin{array}{l} 0 < \rho < \frac{1}{2}, \quad P = 0 \equiv P_1 \\ \frac{1}{2} < \rho < \frac{1}{2}(1+p), \quad P = -4J_A - (1+p)I \equiv P_2 \\ \frac{1}{2}(1+p) < \rho < 1, \quad P = 4[pJ_A - (1-p)J_B] - 2(1+p)I \equiv P_3 \end{array} \right. \\ \text{condition: } I < \min \left\{ -\frac{4}{1+p}J_A, 4(J_A - J_B) \right\} \end{array} \right.$$

$$\left\{ \begin{array}{l} \mathbf{2 \text{ transitions:}} \\ \left\{ \begin{array}{l} 0 < \rho < \frac{1}{2}(1+p), \quad P = P_1 \\ \frac{1}{2}(1+p) < \rho < 1, \quad P = P_3 \end{array} \right. \\ \text{conditions: } \left\{ \begin{array}{l} J_A > \frac{2}{3}J_B \quad \text{and} \\ p > \frac{2J_A - J_B}{J_A - J_B} \equiv p_s \quad \text{and} \\ -\frac{4}{1+p}J_A < I < 2 \left[\frac{p}{1+p}J_A - J_B \right] \end{array} \right. \end{array} \right.$$

$$\left\{ \begin{array}{l} \mathbf{2 \text{ transitions:}} \\ \left\{ \begin{array}{l} 0 < \rho < \frac{1}{2}, \quad P = P_1 \\ \frac{1}{2} < \rho < 1, \quad P = -4[pJ_A + (1-p)J_B + I] = P'_2 \end{array} \right. \\ \text{conditions: } \left\{ \begin{array}{l} J_A < \frac{1}{2}J_B \quad \text{and} \\ p < p_s \quad \text{and} \\ 4(J_A - J_B) < I < -2[pJ_A + (1-p)J_B] \end{array} \right. \end{array} \right.$$

$$\left\{ \begin{array}{l} \mathbf{1 \text{ transition:}} \\ \left\{ \begin{array}{l} 0 < \rho < 1, \quad P = P_1 \\ \text{conditions: } \left\{ \begin{array}{l} p < p_s \quad \text{and} \quad I > -2[pJ_A + (1-p)J_B] \\ \text{or} \\ p > p_s \quad \text{and} \quad I > 2 \left[\frac{p}{1+p}J_A - J_B \right] \end{array} \right. \end{array} \right. \end{array} \right.$$

References

- [1] T. D. Lee and C. N. Yang, Phys. Rev. **87**, 410 (1952).
- [2] L. K. Runnels, in *Phase Transitions and Critical Phenomena*, edited by C. Domb and M. S. Green (Academic Press, London, 1972), Vol. 2, p. 305.
- [3] M. J. de Oliveira and R. B. Griffiths, Surf. Sci. **71**, 687 (1978).
- [4] C. Ebner, C. Rottman, and M. Wortis, Phys. Rev. B **28**, 4186 (1983).
- [5] K. J. Niskanen and R. B. Griffiths, Phys. Rev. B **32**, 5858 (1985).
- [6] J. Lebowitz and O. Penrose, J. Math. Phys. **7**, 98 (1966).
- [7] P. C. Hemmer and G. Stell, Phys. Rev. Lett. **24**, 1284 (1970).
- [8] G. Stell and P. C. Hemmer, J. Chem. Phys. **56**, 4274 (1972).
- [9] G. L. Wilson and G. M. Bell, J. Phys. A **10**, L43 (1977).
- [10] A. P. Vieira and L. L. Gonçalves, Cond. Matt. Phys. (Ukraine) **5**, 210 (1995).
- [11] J. F. Nagle, Phys. Rev. A **2**, 2124 (1970).
- [12] J. Rowlinson and B. Widom, J. Chem. Phys. **52**, 1670 (1970).
- [13] S. Kurioka and K. Ikeda, J. Phys. Soc. Jpn. **57**, 2293 (1988).
- [14] M. F. Thorpe and D. Beeman, Phys. Rev. B **14**, 188 (1976).
- [15] R. Brout, Phys. Rev. **115**, 824 (1959).
- [16] R. M. Mazo, J. Chem. Phys. **39**, 1224 (1963).
- [17] S. Inawashiro, N. E. Frankel, and C. J. Thompson, Phys. Rev. B **24**, 6532 (1981).
- [18] M. Ausloos *et al.*, Phys. Rev. A **28**, 3080 (1983).
- [19] R. R. Singh and J. Kovac, J. Chem. Phys. **90**, 6587 (1989).
- [20] G. Sobotta and D. Wagner, Z. Phys. B **33**, 271 (1979).
- [21] T. Morita, J. Math. Phys. **5**, 1401 (1964).
- [22] M. F. Thorpe, J. Phys. C **11**, 2983 (1978).
- [23] M. Serva and G. Paladin, Phys. Rev. Lett. **70**, 105 (1993).
- [24] See e.g. K. Huang, *Statistical Mechanics, 2nd ed*(John Wiley & Sons, New York, 1987), p.153.

Figure captions

Figure 1. (a-c) $\theta \times \alpha$ diagram, where $\theta \equiv k_B T / |J_B|$ is the renormalized temperature and $\alpha \equiv I / |J_B|$, for dilute short-range interactions ($J_A = 0$) with probabilities $p = 0.1$, $p = 0.25$ and $p = 0.5$, respectively. Continuous curves represent critical temperatures (θ_c and θ'_c) of the phase transitions, while triple point temperatures (θ_t) are shown as dotted curves. Curves for θ'_c and θ_t coincide at point P_{ct} , whose α coordinate (α_{ct}) is shown in (d) as a function of p .

Figure 2. (a) Isotherms $P^* \times \rho$ (continuous curves), where $P^* \equiv P / |J_B|$ is the renormalized pressure, and coexistence curves (dotted curves) for dilute short-range interactions ($J_A = 0$), $p = 0.1$ and $\alpha = 1.5$; (b) Phase diagram $P^* \times \theta$ showing close-packed (CP), liquid (L) and gas (G) phases. Continuous curves correspond to first-order transitions terminating at the critical temperatures θ_c and θ'_c .

Figure 3. (a) The same as in Fig. 2(a) for $\alpha = 2.2$; (b) The same as in Fig. 2(b), but with a triple point indicating coexistence of the three phases.

Figure 4. (a) The same as in Fig. 2(a) for $\alpha_{ct} \simeq 2.4297$; (b) Phase diagram showing the coincidence of the triple point (temperature θ_t) and the critical point of the liquid-close-packed (temperature θ'_c).

Figure 5. $\rho \times \theta$ projections of the coexistence surface for $\delta = 1$ ($\delta \equiv J_A / |J_B|$), $p = 0.07$ and (a) $\alpha = 1.13$ and (b) $\alpha = 1.129$. The triple point present in (a), whose temperature is θ_t , is suppressed in (b), where a coexistence “bubble” can be observed, as indicated by the arrows.

Figure 6. $\theta \times \alpha$ diagram for $\delta = 1$ and $p = 0.07$. The inset shows the breaking and reentrant behavior of the θ_c curve, as well as the existence of the new points P''_{ct} and P'''_{ct} , extremes of a new triple point line (dotted). The θ'_c curve is omitted from the inset for clarity.

Figure 7. $\theta \times \alpha$ diagram for $\delta = 2$ and $p = 0.1$. The four (dotted) triple point lines intersect at the quadruple point P_q .

Figure 8. Phase diagram for $\delta = 2$, $p = 0.08$ and (a) $\alpha = 2.3$, (b) $\alpha_q \simeq 2.3277$ and (c) $\alpha = 2.35$. Two triple points are evident in (a) and (c), while the quadruple point is present in (b). In all cases the axes intervals are $0 \leq \theta \leq 2.4$ and $0 \leq P^* \leq 0.8$.

Figure 9. $\rho \times \theta$ ($\theta \equiv k_B T / |J_B|$) projections of the coexistence surfaces for $\delta = 2$, $p = 0.08$ and (a) $\alpha = 2.3$, (b) $\alpha_q \simeq 2.3277$ and (c) $\alpha = 2.35$. The broken lines indicate the triple point temperatures in (a) and (c), and the quadruple point temperature in (b).

Figure 10. (a-c) $\theta \times \alpha$ diagram, where $\theta \equiv k_B T / |J_B|$ is the renormalized temperature and $\alpha \equiv I / |J_B|$, for the case $J_A = \frac{3}{10} J_B < 0$ ($\delta = -\frac{3}{10}$) with probabilities $p = 0.25$, $p = 0.25$ and $p = 0.5$, respectively. Continuous curves represent critical temperatures (θ_c and θ'_c) of the phase transitions, while triple point temperatures (θ_t) are shown as dotted curves. Coordinates α_{ct} and α'_{ct} of points P_{ct} and P'_{ct} , as well as values α_2 and α_3 at which triple point temperatures become zero, are shown in (d) as a function of p . Notice that, while α_{ct} goes to $\alpha_{tr} \simeq 3.1532$ as $p \rightarrow 0$, α'_{ct} goes to $|\delta| \alpha_{tr} \simeq 0.9459$ as $p \rightarrow 1$, as expected.

Figure 11. (a) $P^* \times \rho$ isotherms (solid lines) and coexistence curves (dotted lines) for $\delta = -0.3$, $p = 0.5$ and $\alpha = 0.8$; (b) $P^* \times \theta$ phase diagrams showing the various transition lines and critical temperatures; (c) $\rho \times \theta$ projections of the coexistence curves shown in (a).

Figure 12. The same as in Fig. 11 for $p = 0.75$. Notice in (b) and (c) the existence of a triple point.

Figure 13. $\theta \times \alpha$ diagram for $\delta = -0.6$ and $p = p^\dagger = 0.5$, showing the critical temperatures (solid lines) and triple point temperatures (dotted lines).

Figure 14. (a) $P^* \times \rho$ isotherms (solid lines) and coexistence curves (dotted lines) for $\delta = -0.6$, $p = 0.5$ and $\alpha = 1.45$; (b) $P^* \times \theta$ phase diagrams showing the various transition lines, critical temperatures and the triple point.

Figure 1. A. P. Vieira and L. L. Gonçalves.

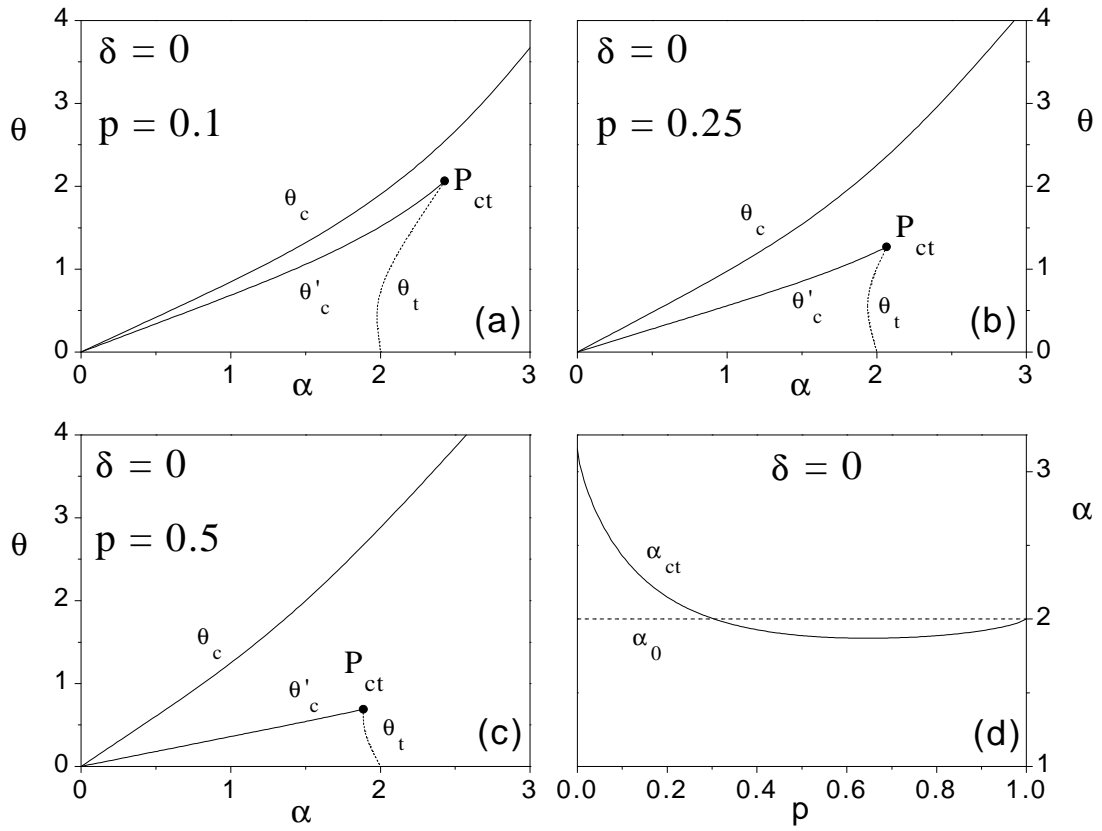


Figure 2. A. P. Vieira and L. L. Gonçalves.

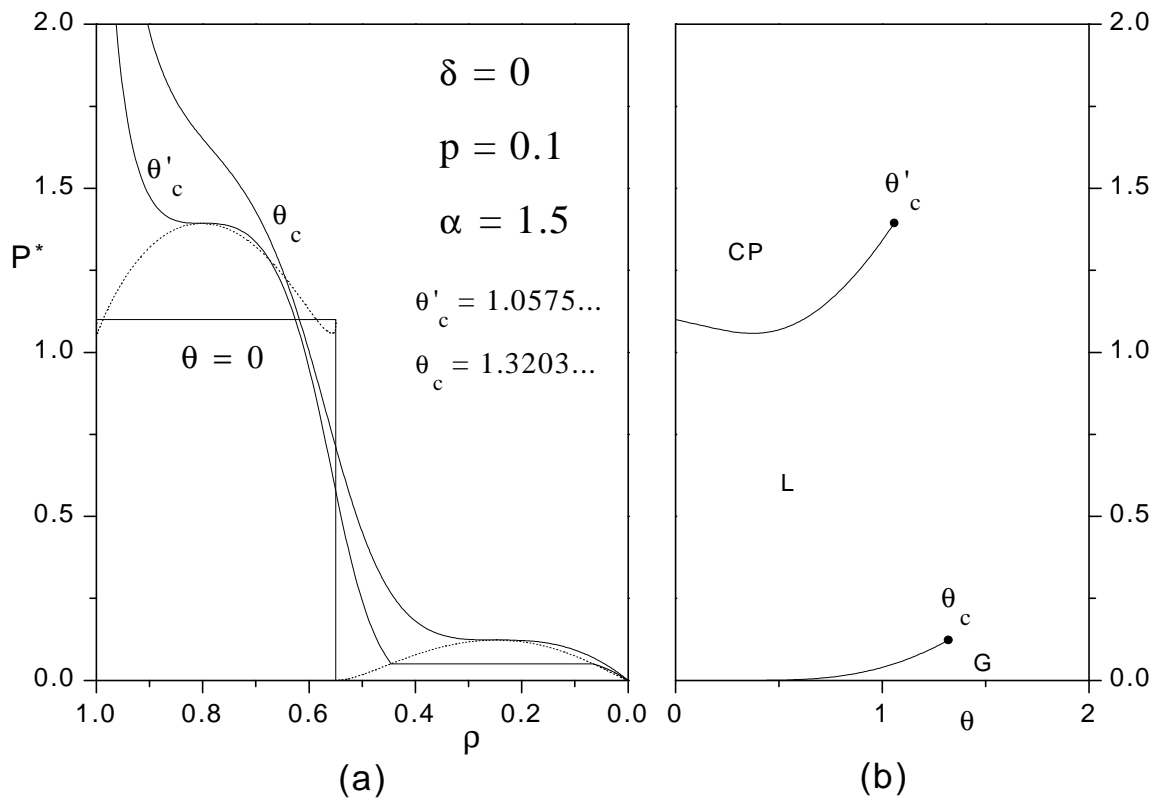


Figure 3. A. P. Vieira and L. L. Gonçalves.

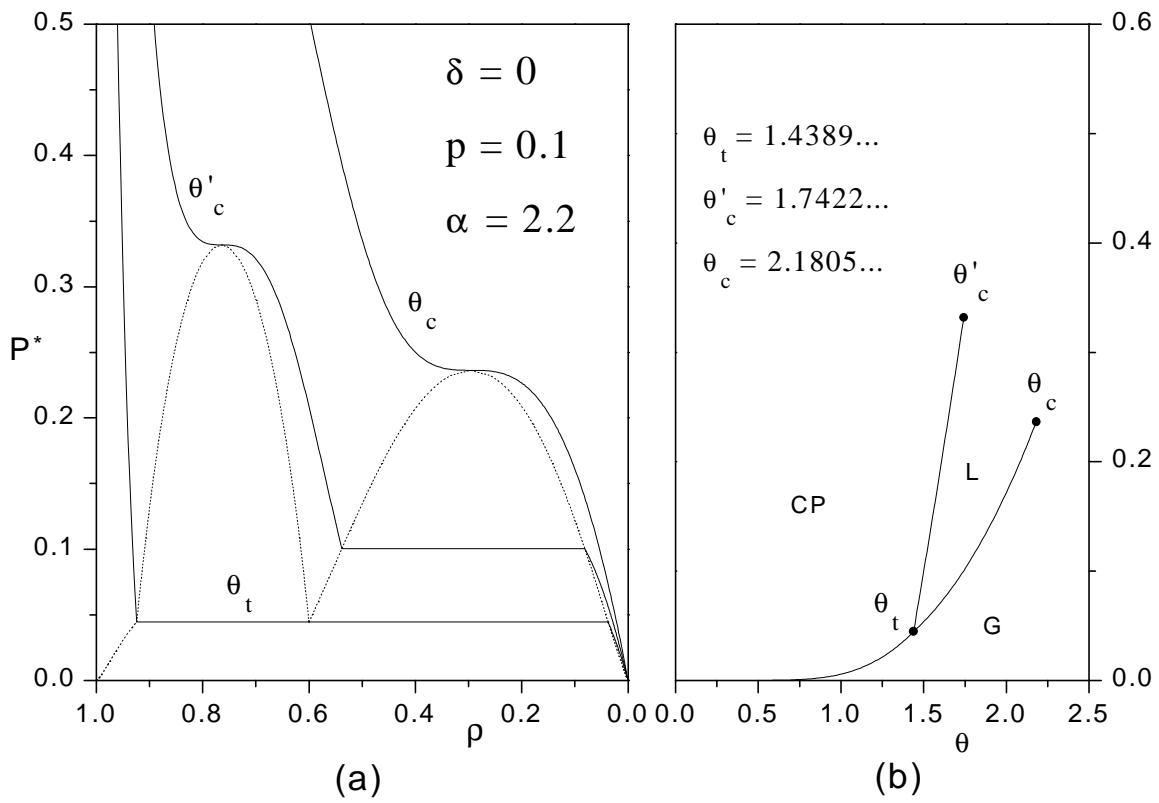


Figure 4. A. P. Vieira and L. L. Gonçalves.

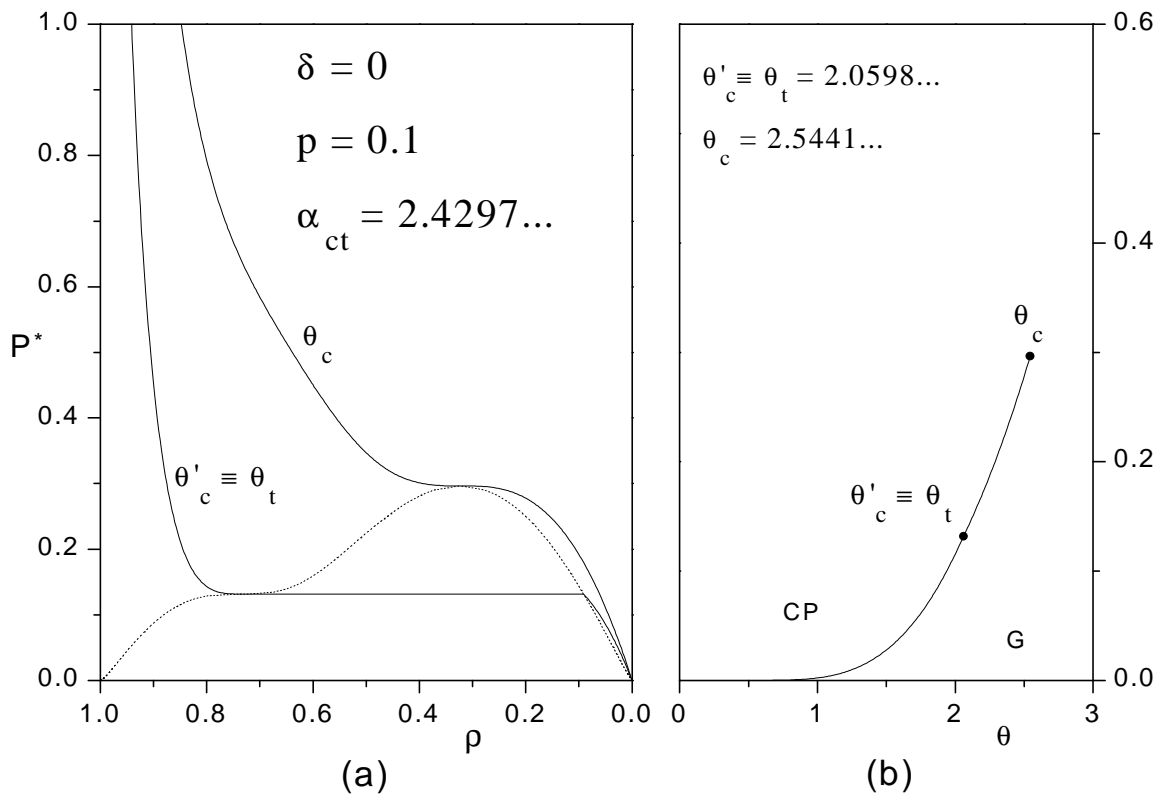


Figure 5. A. P. Vieira and L. L. Gonçalves.

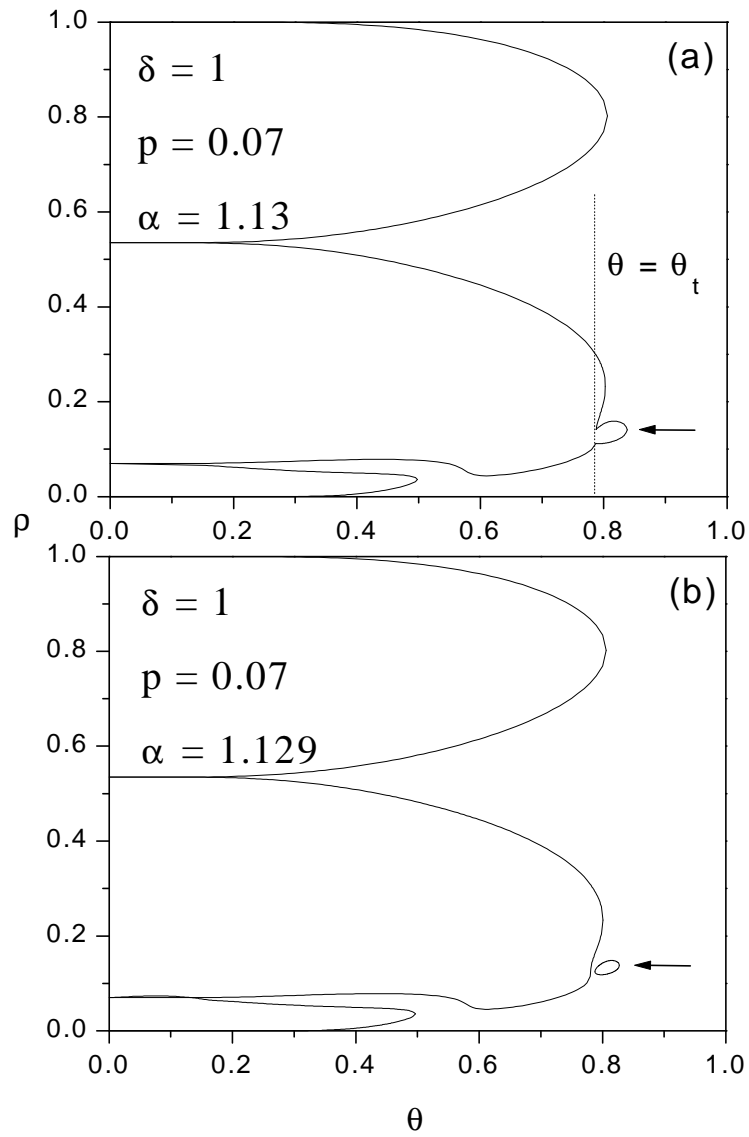


Figure 6. A. P. Vieira and L. L. Gonçalves.

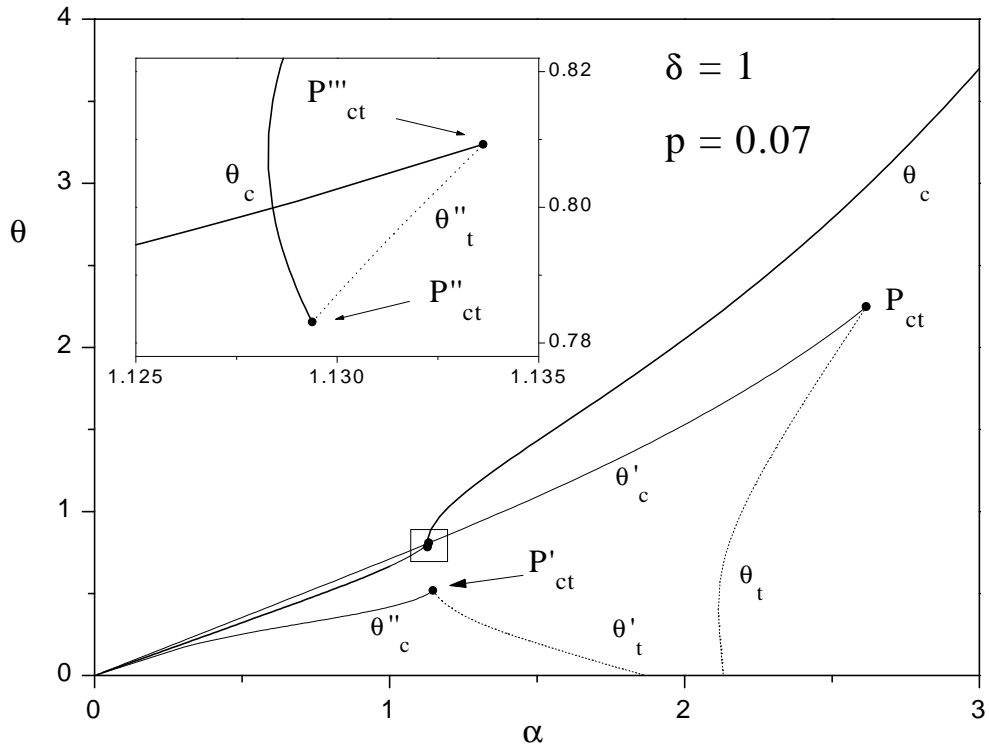


Figure 7. A. P. Vieira and L. L. Gonçalves.

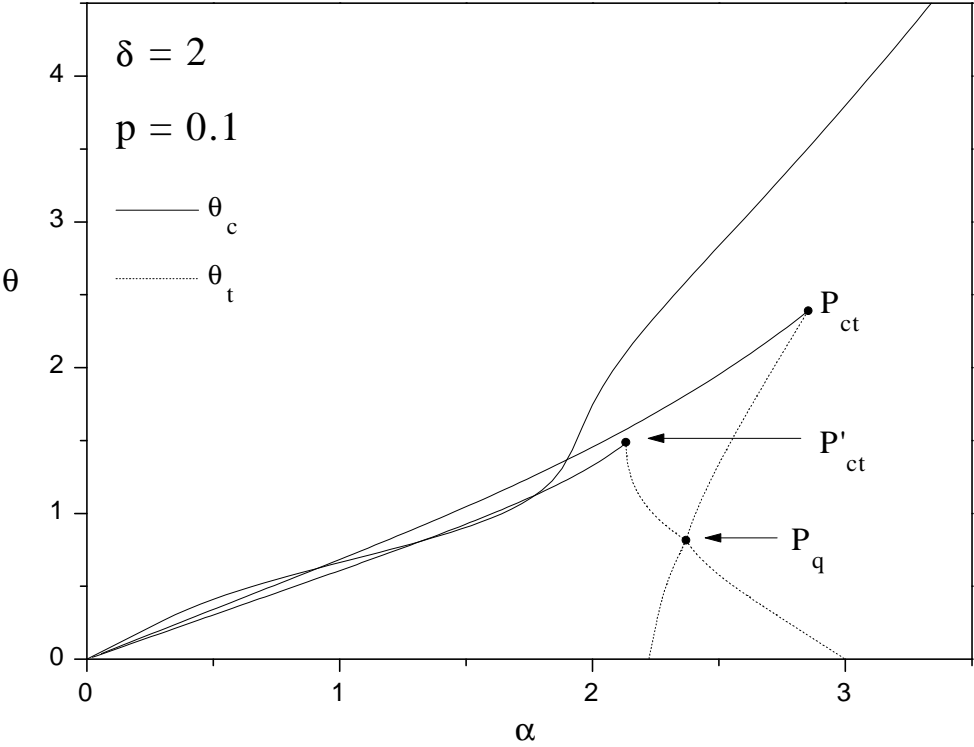


Figure 8. A. P. Vieira and L. L. Gonçalves.

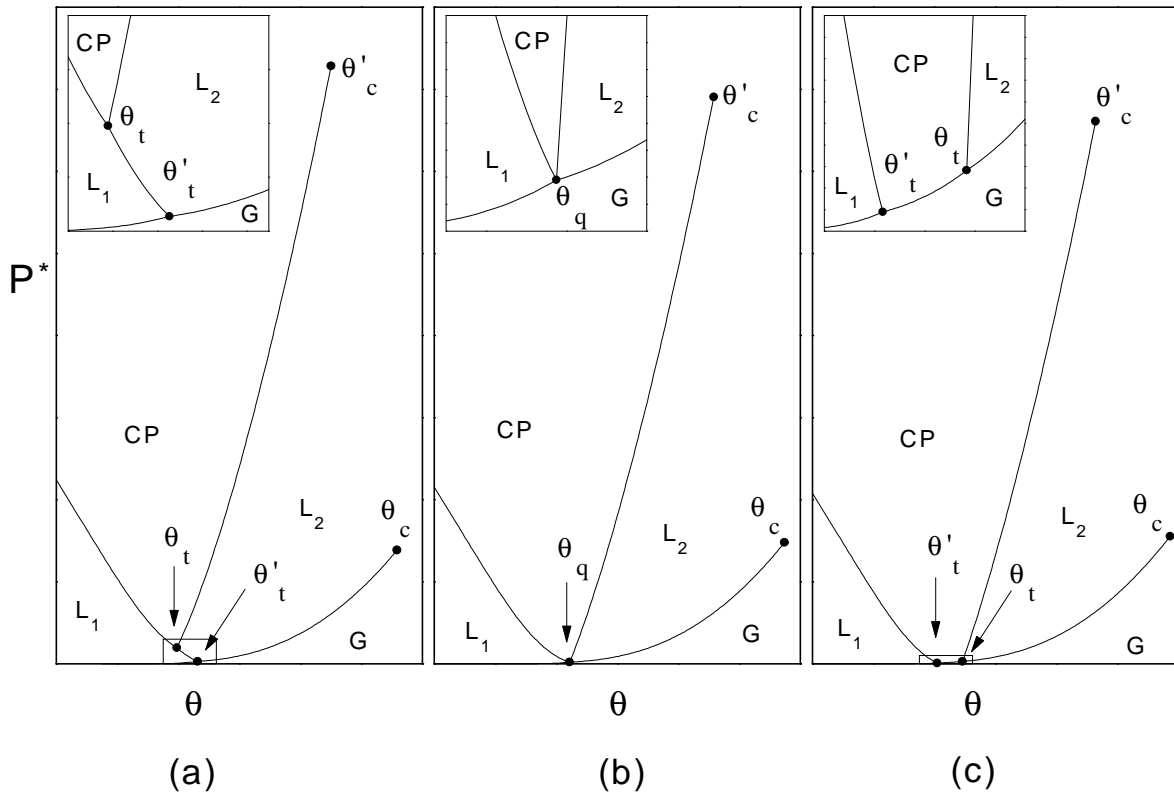


Figure 9. A. P. Vieira and L. L. Gonçalves.

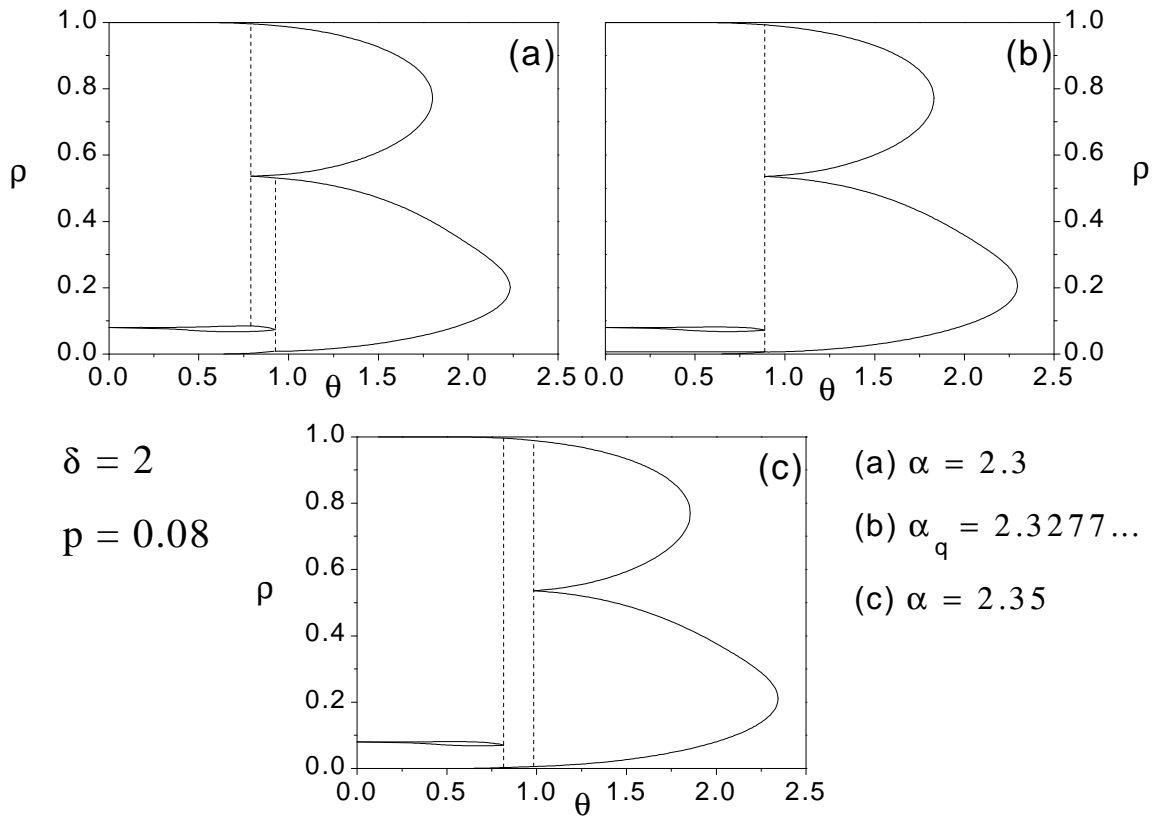


Figure 10. A. P. Vieira and L. L. Gonçalves.

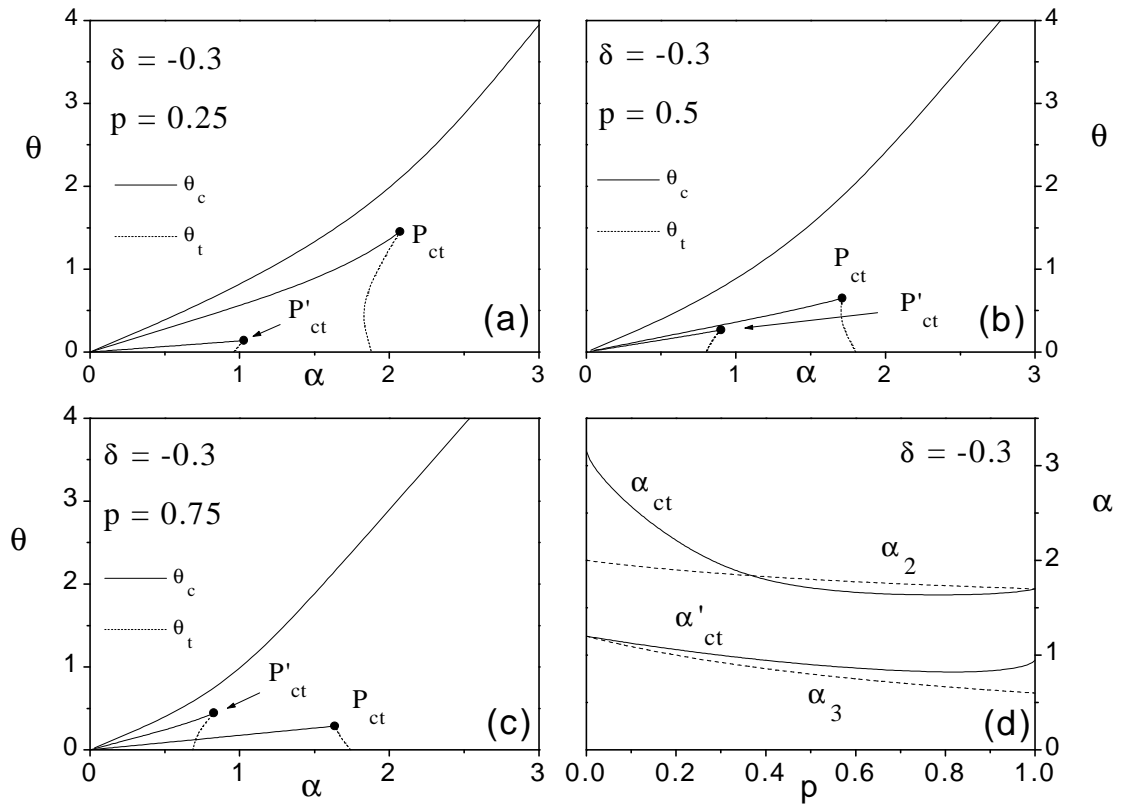


Figure 11. A. P. Vieira and L. L. Gonçalves.

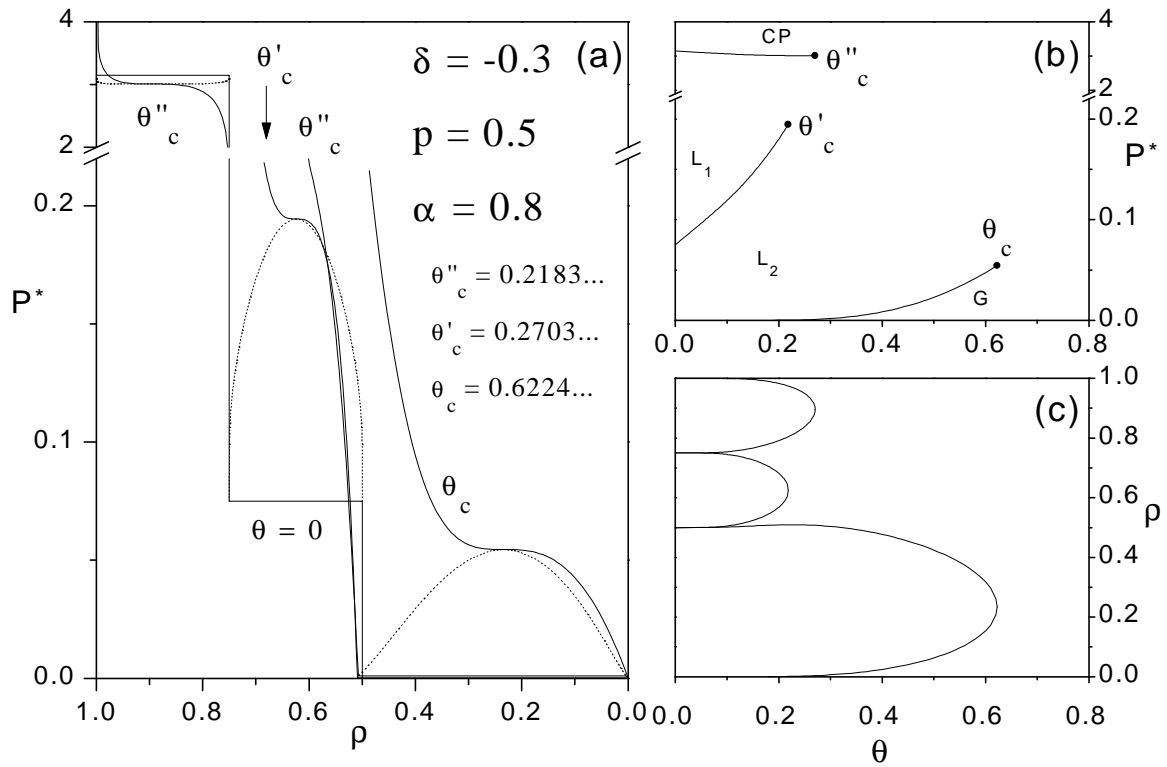


Figure 12. A. P. Vieira and L. L. Gonçalves.

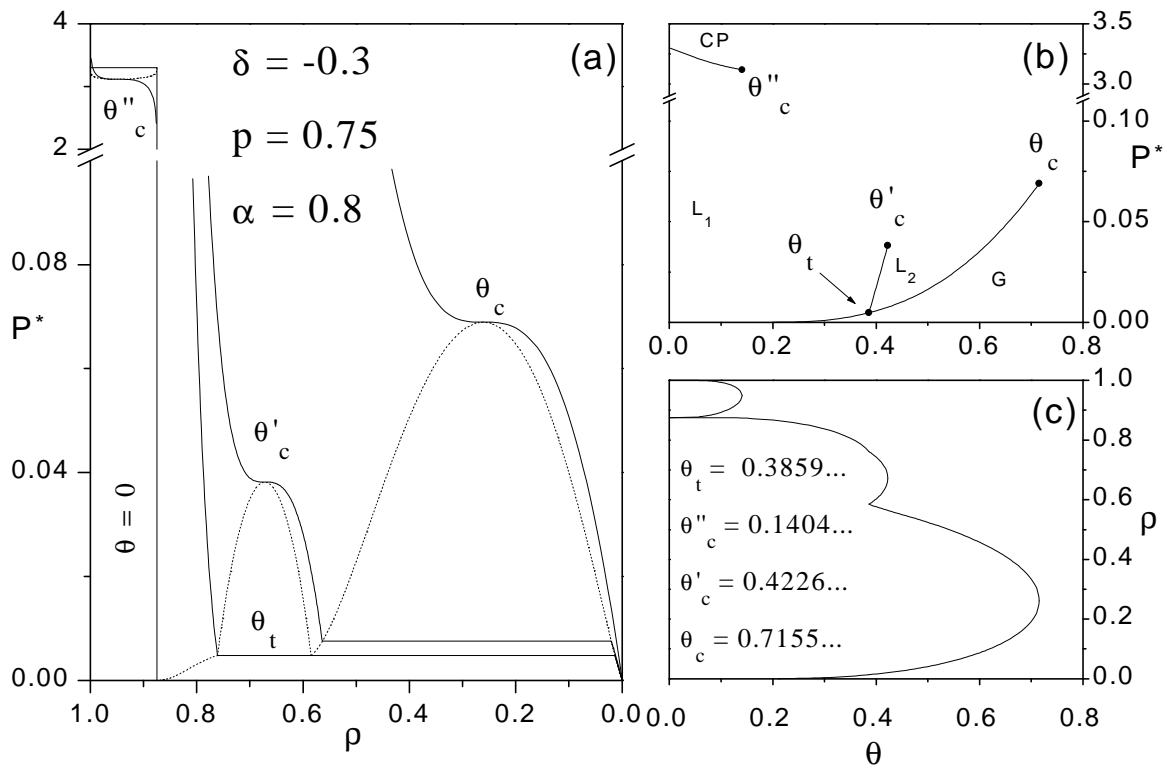


Figure 13. A. P. Vieira and L. L. Gonçalves.

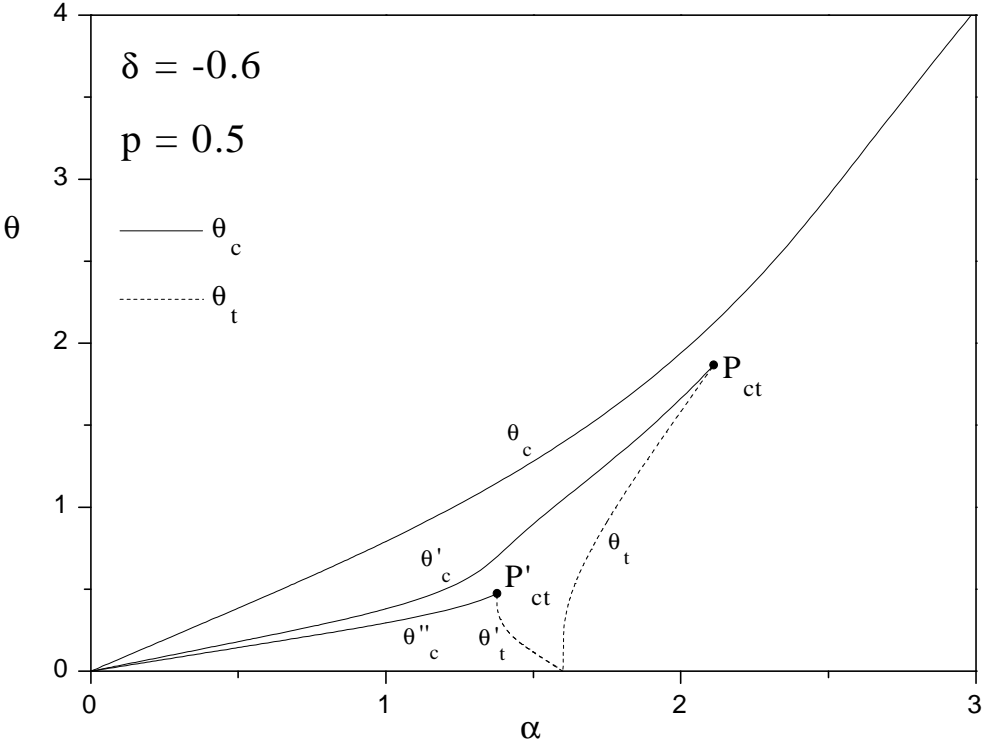


Figure 14. A. P. Vieira and L. L. Gonçalves.

